Modeling of the Contact between the Metal Tip and n-type Semiconductor as a Schottky Barrier and Tunneling Current Calculation

Dongwook Go*
Institute of Solid State Physics, Technical University of Graz, Petersgasse 16, 8010 Graz, Austria
(Dated: February 3, 2013)

The contact between the metal tip and n-type semiconductor contact is modeled as a Schottky barrier and IV curves are calculated for various parameters. It is observed that when the thermionic current dominates the tunneling current contribution (high T, large a, small U_0, large ξ) the IV curve just follows the usual diode behavior. However, when tunneling current dominates (low T, small a, large U_0, small ξ), the reverse current starts to appear and thereby reverse the rectifying behavior of the diode.

INTRODUCTION

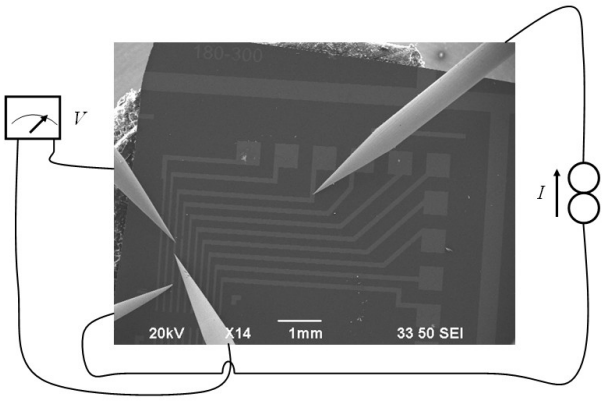

FIG. 1. Four-point measurement is widely used to measure the resistivity of the sample. (Source : http://lamp.tu-graz.ac.at/ hadley/sem/index/index.php)[1]

Nowadays, electron devices tend to have small sizes (a few nanometers to a few microns). In order to investigate the small size devices, in TU Graz, a scanning electron microscope (SEM) is used with a sharp metal tip which can move accurately within a few nanometers[1]. With the sharp metal tip, the current and the voltage are measured. For example, the resistivity of the sample can be measured through the four-point measurement (Fig.1). Also, the electron beam induced current (EBIC) method is commonly used to identify buried junctions or defects in semiconductors, or to examine minority carrier properties (Fig.2). As mentioned above, many experiments depend on the tip measurement, so it is important to understand the contact between the tip and the sample.

However, little is known about the properties of the contact between the tip and the sample although many experiments depend on the tip measurement, so the research on the properties of the contact has to be done. In two-point measurement of the IV curve, most of the resistance comes from the contact, and the IV curve shows that the resistivity becomes smaller as the bias voltage increases for both forward and reverse bias voltages. To

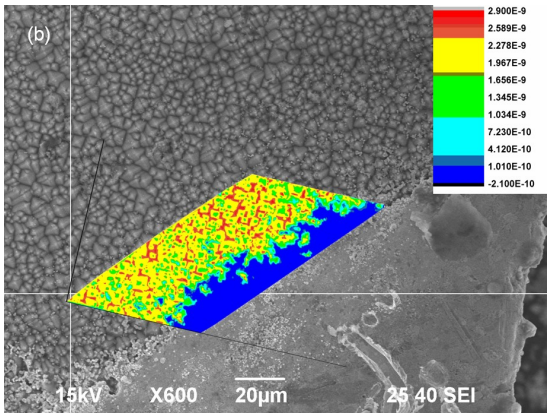

FIG. 2. EBIC method is used to study buried junctions or defects in semiconductors. (Source : http://lamp.tu-graz.ac.at/ hadley/sem/index/index.php)[1]

explain the shape of the IV curve, the theoretical model is suggested in this paper and the IV characteristic is explained with the suggested model.

In the theoretical model, Schottky contact is formed at the contact between the metal tip and the n-type semiconductor sample. Assuming that the charge density is constant through the depletion layer, the potential barrier can be calculated, which shows a $V \sim r^{-1}$ behavior. Then, the Schrodinger equation is solved with the calculated potential function. In this step, the transmission coefficient is obtained. Finally, the current density is calculated using the calculated transmission coefficient and the Fermi-Dirac distribution function.

Meanwhile, to be sure about the calculation, the current density was calculated for the square barrier potential, which agrees well with the previous study[2].

For the spherical shape Schottky barrier, the diode-like behavior is observed when the thermionic current dominates the tunneling current, which can be understood in general terms like in many other semiconductor textbooks. However, when the tunneling current is a major source of the current, it is observed that the reverse current starts to appear, so the rectifying behavior of the diode is reversed.

THEORY AND MODEL

A. Modeling of the Contact : Spherical Shape Schottky Barrier

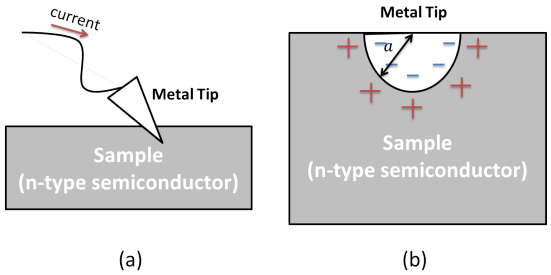

FIG. 3. (a) Geometry of the contact between the tip and the sample. (b) The model is simplified to have a spherical shape contact.

In the theoretical model, there is a metal tip, and the sample is assumed to be a n-type semiconductor. The analysis of a p-type semiconductor is almost the same as the n-type one. The usual geometry of the tip measurement is like Fig.3. The tip and the n-type semiconductor sample become contact each other, and the Schottky contact is formed if the Fermi energy of the n-type semiconductor is higher than that of metal tip. The electron moves to the metal tip side, so the positively charged depletion region is formed around the tip. In the model, I assumed for the mathematical simplicity that the shape of the contact is spherical shape with a radius a.

In Fig.4, the energy level diagram of Schottky contact is illustrated[3]. Before the contact is formed, the Fermi energy of the n-type semiconductor is higher than that of the metal tip. When the two become contact each other, small amount of electron moves to the metal side, so the Fermi energies of both sides become equal and the Schottky barrier is formed. When the bias voltage is applied, the difference of the Fermi energies becomes eV.

B. Potential Barrier Calculation through the Poisson Equation

For the simplicity, I assumed that the charge density at the depletion layer is constant ($\rho = eN_d$), which is called the depletion approximation[4]. Then, the Poisson equation

$$\nabla^2 V(\vec{r}) = -\frac{\rho}{\epsilon} \tag{1}$$

is to be solved. Here, the electric potential is radially symmetric ($V(\vec{r}) = V(r)$), so the Poisson equation becomes

$$\frac{1}{r^2}\frac{d}{dr}\left(r^2\frac{d}{dr}V(r)\right) = -\frac{eN_d}{\epsilon}. \tag{2}$$

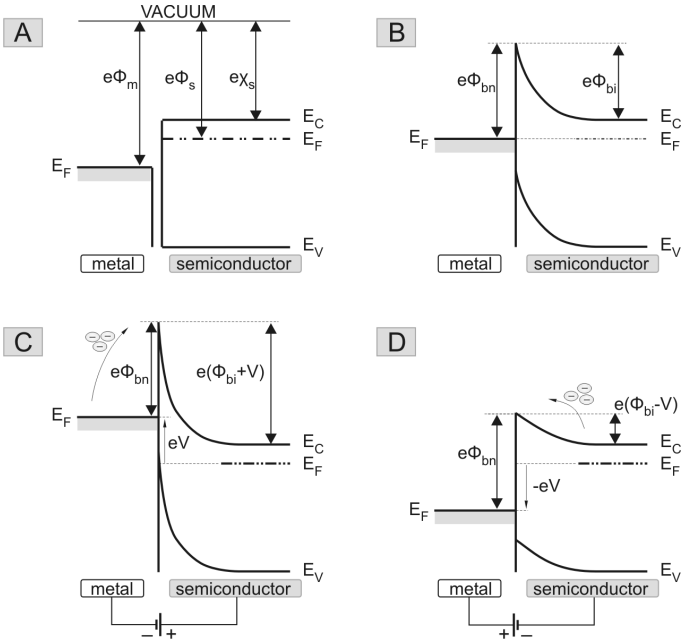

FIG. 4. Before the contact is formed, Fermi energy of the n-type semiconductor is higher than that of metal tip. When the two become contact each other, small amount of electron moves to the metal side, so the Fermi energies of both sides become equal and the Schottky barrier is formed. When the bias voltage is applied, the difference of Fermi energies becomes eV. (Source : http://web.tiscali.it/decartes/phd_html/node3.html)[3]

If we multiply r^2 and integrate,

$$r^2\frac{d}{dr}V(r) = -\frac{eN_d r^3}{3\epsilon} + C_1 \tag{3}$$

and, if we divide by r^2 and integrate, we arrive at the general form of the potential.

$$V(r) = -\frac{eN_d r^2}{6\epsilon} - \frac{C_1}{r} + C_2 \tag{4}$$

The coefficient C_1 can be obtained by using the fact that at the end of the depletion layer($r = r_d$) the electric field vanishes,

$$E(r_d) = -\frac{d}{dr_d}V(r_d) = -\frac{eN_d r_d}{3\epsilon} + \frac{C_1}{{r_d}^2} \tag{5}$$

so, $C_1 = eN_d r_d^3/3\epsilon$. The coefficient C_2 can be obtained by setting the ground potential as $V(r_d) = 0$, so $C_2 = 3N_d r_d^2/2\epsilon$. Therefore, the electric potential of the spherical Schottky contact is

$$V(r) = \begin{cases} V_{bi} & (r < a) \\ \frac{eN_d}{6\epsilon}\left(3{r_d}^2 - r^2 - \frac{2{r_d}^3}{r}\right) & (a \le r \le r_d) \\ 0 & (r \ge r_d) \end{cases} \tag{6}$$

with the constraint $V(a) = V_s + V_{bi}$, where V_s is the intrinsic potential drop at the contact, and V_{bi} is the bias voltage applied to the metal side.

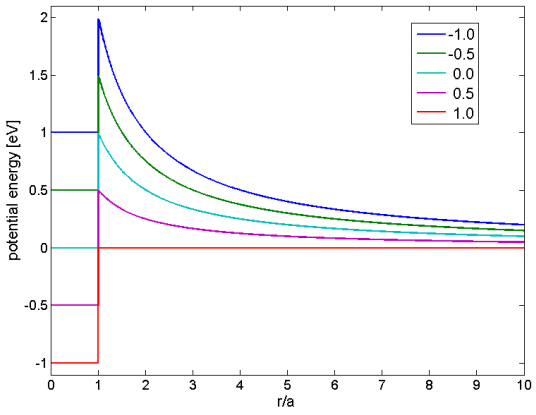

FIG. 5. Potential energy ($U = -eV$) profile for various V_{bi} values. When negative(positive) voltage is applied the barrier becomes higher(lower) and thicker(thinner). The intrinsic voltage drop (V_s) is set to -1 V.

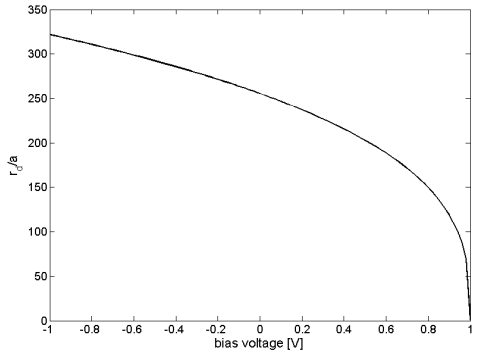

FIG. 6. As the metal side becomes more negatively biased the depletion layer radius (r_d) increases. The intrinsic potential drop at the barrier (V_s) is set to be -1 V.

At Fig.6, potential energy profile for various bias voltage (V_{bi}) is shown. When negative voltage is applied the barrier becomes higher and thicker, and vice versa. It was assumed that $N_d = 10^{15}$ cm^{-3}, and $a = 1nm$. Also, at the Fig.5, the radius of the depletion layer (r_d) is calculated for various bias voltages. It can be seen that as the bias voltage becomes negative the depletion layer thickness increases.

C. Schrodinger Equation and Transmission Probability

In general, the transmission probability can be calculated by solving time-independent Schrodinger equation.

$$-\frac{\hbar^2}{2m^*}\frac{d^2}{dx^2}\psi_E(x) + U(x)\psi_E(x) = E\psi_E(x) \tag{7}$$

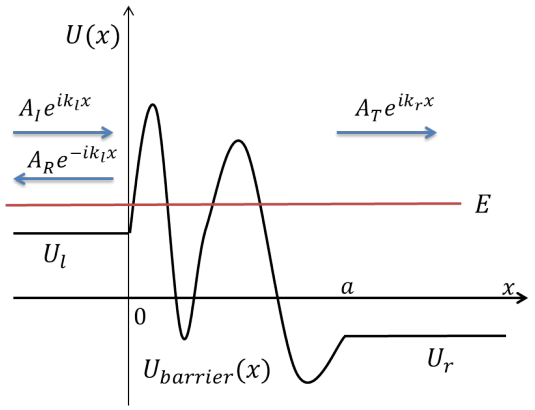

FIG. 7. Schematic diagram of the potential barrier and the tunneling phenomenon. When an incident wave ($A_I e^{ik_l x}$) approaches to the barrier, a part is reflected back ($A_R e^{-ik_l x}$) and the other part transmits through the barrier ($A_T e^{ik_r x}$).

where m^* is an effective mass of the electron.

Suppose the system where the potential is constant at a region $x < 0$ and $x > a$ and in between there's a potential barrier. Here, $U_l(U_r)$ is a constant potential on left(right) side.

$$U(x) = \begin{cases} U_l & (x < 0) \\ U_{barrier}(x) & (0 < x < a) \\ U_r & (x > a) \end{cases} \tag{8}$$

It is known that the solution under the constant potential is a plane wave. So we can write the solution as a combination of the incident wave, the reflected wave, and the transmitted wave

$$\psi_E(r) = \begin{cases} A_I(E)e^{ik_l x} + A_R(E)e^{-ik_l x} & (x < 0) \\ A_T(E)e^{ik_r x} & (x > a) \end{cases} \tag{9}$$

where

$$k_l = \frac{\sqrt{2m^*(E - U_l)}}{\hbar} \tag{10}$$

and

$$k_r = \frac{\sqrt{2m^*(E - U_r)}}{\hbar}, \tag{11}$$

which are the wave numbers on the left(right) side. A schematic diagram is shown in Fig.(7).

With the initial condition

$$\begin{cases} \psi(x = a) = e^{ik_r x} \\ \left(\frac{\partial \psi}{\partial x}\right)_{x=a} = ik_r e^{ik_r x} \end{cases} \tag{12}$$

we can integrate the Eq.(7) numerically and get ψ and $d\psi/dx$ at the point $x = 0$. Here we can impose the condition $A_T = 1$ since only the relative values of coefficients are physically meaningful. The coefficients are

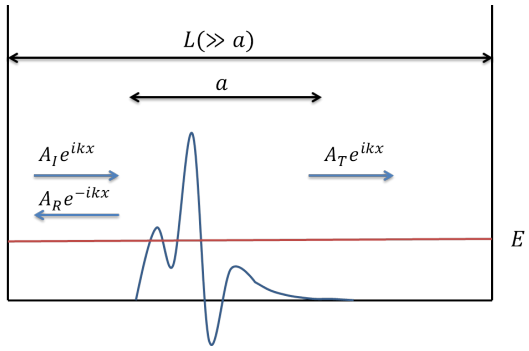

FIG. 8. The periodic boundary condition assumes that the wave function is the same in every period $L(\gg a)$.

just needed to meet the constraint, $|A_I|^2 = |A_R|^2 + |A_T|^2$. Therefore, we can calculate A_I and A_T as follows.

$$\begin{cases} A_I(E) = \frac{1}{2}\psi(0) + \frac{1}{2ik}\left(\frac{\partial\psi}{\partial x}\right)_{x=0} \\ A_T(E) = \frac{1}{2}\psi(0) - \frac{1}{2ik}\left(\frac{\partial\psi}{\partial x}\right)_{x=0} \end{cases} \tag{13}$$

Then, we can calculate the transmission probability as

$$T(E) = 1 - \left|\frac{A_R(E)}{A_I(E)}\right|^2. \tag{14}$$

D. Current Density

Current density can be calculated from the tunneling probability and the Fermi-Dirac distribution[4]. For the convenience in counting the number of states, periodic boundary condition is imposed. The boundary condition assumes that the wave function is same in every space period L, which means that the wave function has a period L. The period L is assumed to be much larger than the system itself ($L \gg a$).

Let's consider the system in Fig.8. The incident wave coming from the left side ($A_I e^{ikx}$) is reflected ($A_R e^{-ikx}$) and transmitted ($A_T e^{ikx}$) at the potential barrier. If we set $A_I = 1$, the normalized wave function is given by

$$\psi_k(r) = \begin{cases} \frac{1}{\sqrt{L}}\left(e^{ikx} + A_R(k)e^{-ikx}\right) & (left\ side) \\ \frac{1}{\sqrt{L}}A_T(k)e^{ikx} & (right\ side) \end{cases}. \tag{15}$$

so when the boundary condition ($\psi_k(x+L) = \psi_k(x)$) is imposed, the possible k values form a set of discrete numbers, and the unit length of k-space becomes $2\pi/L$

$$k = \frac{2\pi}{L}m,\ m \in Z \tag{16}$$

where Z is the set of integers.

The current density of the quantum state with the wave number k is the electron charge $(-e)$ times the probability current.

$$J_k(L \to R) = -\frac{e\hbar}{2m^* i}\left[\psi_k^*\frac{\partial\psi_k}{\partial x} - \psi_k\frac{\partial\psi_k^*}{\partial x}\right] = (-e)\frac{T(k)}{L}\frac{\hbar k}{m} \tag{17}$$

The overall current density of the left-incoming case is sum over the all possible k values times Fermi function factor.

$$J(L \to R) = 2\sum_k (-e)\frac{T(k)}{L}\frac{\hbar k}{m} f_L(k)\left(1 - f_R(k)\right) \tag{18}$$

where the first Fermi function factor ($f_L(k)$) is the probability that the state k is occupied on the left side of the barrier, and the second factor $(1 - f_R(k))$ is the probability that the state k is empty on the right side of the barrier. Meanwhile, the factor 2 in the front comes from the spin degree of freedom for each k values. If we change it into the integral representation, it becomes

$$J(L \to R) = \frac{2}{(2\pi/L)}\int_k dk(-e)\frac{T(k)}{L}\frac{\hbar k}{m} f_L(k)\left(1 - f_R(k)\right). \tag{19}$$

The last step is to change the integral variable into the energy, $E = \hbar k^2/2m$, and the integral becomes

$$J(L \to R) = -\frac{4e}{h}\int_E T(E) f_L(E)(1 - f_R(E))dE. \tag{20}$$

Similarily, the current density which flows from the right side to the left side is

$$J(R \to L) = -\frac{4e}{h}\int_E T(E) f_R(E)(1 - f_L(E))dE. \tag{21}$$

Therefore the total current is the difference of the two contributions.

$$J_{total} = \frac{4e}{h}\int_E T(E)(f_R(E) - f_L(E))dE. \tag{22}$$

EXPERIMENT AND RESULT

Experimental result was referred from Alexander Schnabel and Stephan Stonica's report of the class, experimental laboratory exercise, in TU Graz[4].

The setup for the experiment is shown in Fig.9. A part of the n-doped silicon wafer is placed between the two copper plates. The sample was proton-doped silicon wafer produced by Infineonn named P570_530. Four tips driven by the macro manipulator are placed on the silicon. All the tips and copper plates are enumerated from 1 to 6. The tip 1,2, and 3 are composed of tungsten, and 4 is copper-beryllium. The copper plates are enumerated as 5 and 6.

A series of two-point measurements between the tips or between the tip and the copper plates has been carried out, and the IV curve is shown in Fig.10. It is observed

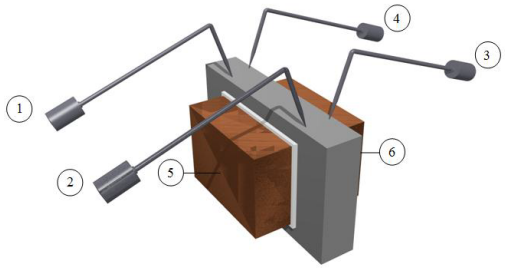

FIG. 9. Setup for the measurement. 1-3 Tungsten Tips, 4 Copper-Beryllium tip, 5,6 Copper-plates.

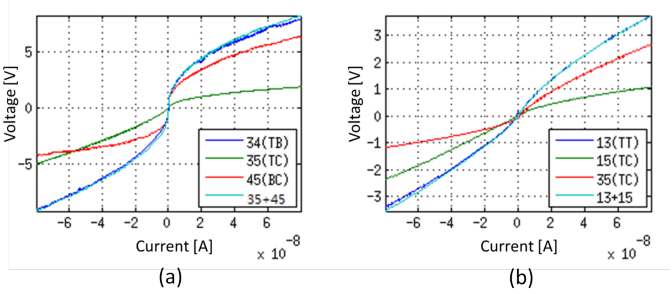

FIG. 10. The IV curves for the tip-semiconductor contact.(blue : tip-tip, green : tip1-cu, red : tip2-cu, turquoise : red and green added) On the left side one tungsten and one copper-beryllium tip is used, while two tungsten tips were used in the right.

from the IV curve that the resistivity becomes smaller as the magnitude of the bias voltage increases. In Fig.10-(a), the IV curve of 34 is compared with the sum of the two curves, 35+45, which gives almost the same result. This suggests that the most of the resistivity comes from the tip-semiconductor contact, and that the resistivity which comes from the contact between the copper plate and the semiconductor is small. The same thing can also be seen in Fig.10-(b).

Therefore, it is concluded that the resistivity that comes from the tip-semiconductor contact shows nonlinear behavior, where the resistivity becomes smaller as the magnitude of the bias voltage increases. In the next section, the IV curve at the tip-semiconductor contact is numerically calculated, and this behavior is explained within the theoretical model.

NUMERICAL CALCULATION RESULT

Using the theory and the model discussed before, the IV curves are calculated for both square and Schottky potential barrier.

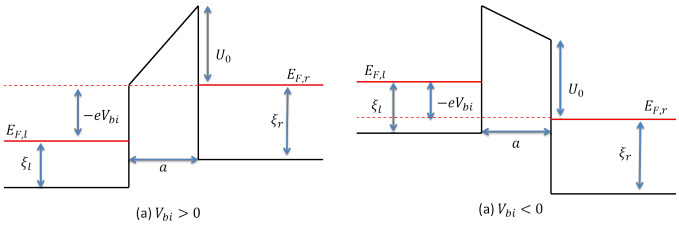

FIG. 11. Energy band diagram of the square potential barrier when (a) $V_{bi} > 0$ and (b) $V_{bi} < 0$.

A. Square Barrier

The parameters for the calculations are defined as below (See Fig.11) :

Barrier Height	U_0
Barrier Width	a
Fermi Energy on the Left/Right	$E_{F,l}/E_{F,r}$
Conduction Band Bottom on the Left/Right	$E_{C,l}/E_{C,r}$
$E_F - E_C$	ξ_l/ξ_r
Bias Voltage	V_{bi}

As the two different materials become contact each other, the Fermi energies of two different materials become the same. Then, if a bias voltage is applied, the Fermi energies becomes different as Eq.(25), so electrons can flow.

$$E_{F,r} - E_{F,l} = -eV_{bi} \tag{23}$$

Moreover, the wave vectors on the left and right sides are given by

$$k_l = \sqrt{\frac{2mE}{\hbar^2}}, \tag{24}$$

and

$$k_r = \sqrt{\frac{2m(E + \xi_l - \xi_r + eV_{bi})}{\hbar^2}}, \tag{25}$$

where E is the energy of the electron which is set to be zero at the bottom of the conduction band on the right side.

The first thing to note is the dependence of the barrier thickness, a. In Fig.12, IV curves were calculated for the barrier thicknesses 10^{-11} m, 10^{-10} m, 10^{-9} m, and 10^{-8} m. The other conditions were set to be the same ($U_0 = 2$ eV, $\xi_l = \xi_r = 2$ eV, $T = 300$ K). It can be seen that as the barrier thickness becomes smaller it becomes to follow the Ohmic behavior while the curves have the bigger curvature when the barrier becomes thick. When the barrier is thick it's hard for electrons to penetrate through the tunneling, so the electrons can tunnel through the barrier only when the high enough bias voltage is applied .

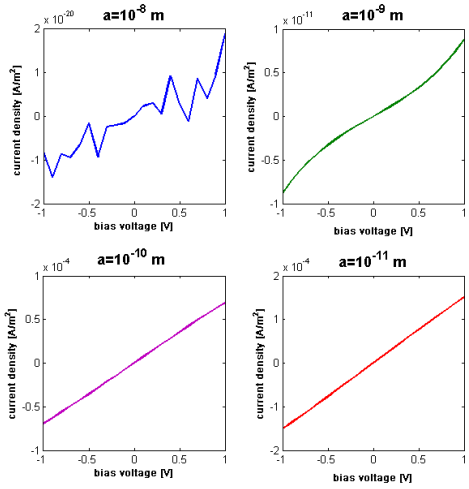

FIG. 12. IV curves for various values of barrier thickness. As the barrier thickness become smaller it becomes to follow the Ohmic behavior while the curves have bigger curvature when the barrier is thick.

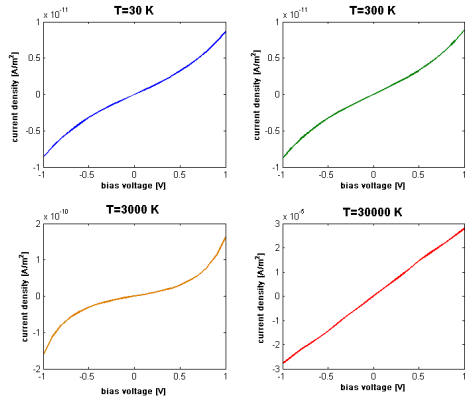

FIG. 13. Temperature dependence of the IV curves. In extremely high temperature the Ohmic behavior is observed. While in low temperature regime, the curvatures of the curve can be seen, especially for the $T = 3000\ K$ case, which comes from the quantum interference effect.

In Fig.13, a similar trend can also be observed in the calculation for various temperatures (30 K, 300 K, 3000 K, and 30000 K) while all the other conditions were set to be the same ($U_0 = 2\ eV$, $\xi_l = \xi_r = 2\ eV$, $a = 1\ nm$). In extremely high temperature, the IV curve just becomes linear, where the contribution to the current comes mostly from the thermionic emission. While in a low temperature region, like 30 K and 300 K, most of the current comes from the tunneling electrons whose energy is low. An interesting behavior is observed at 3000 K, where the curvature can be seen easily. In this temperature region there are enough electrons whose energy is almost at the tip of the barrier, so they can tunnel easily.

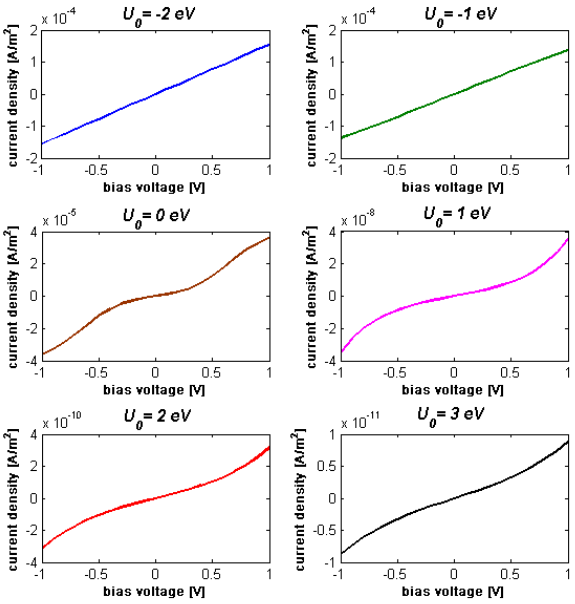

FIG. 14. IV curves for the different U_0 values. It's Ohmic when the height is small and come to have a curvature as the height becomes bigger. Especially for the $U_0 = 0$ case, the funny shape of the curve can be observed since the energy of the electrons is almost at the edge of the barrier.

The electrons in this energy region show the quantum interference effect where incoming wave and reflected wave interfere each other, thus showing a funny shape of the IV curve.

The next thing to note is the barrier height dependence of the IV curves. In Fig.14, IV curves for various barrier height are shown. Here also, the other conditions are set to be the same for each calculation ($T = 300\ K$, $\xi_l = \xi_r = 2\ eV$, $a = 1\ nm$). The first case, $U_0 = -2\ eV$ means the free space, no barrier case. When the barrier height is low the IV curves are linear. As the barrier height increases, the IV curves come to have a curvature, and an interesting IV curve can be observed for the $U_0 = 0$ case where the electrons have an energy that is almost equal to the edge of the barrier, so the interference occurs.

Finally, the IV curves for various ξ_r values (0-4 eV) are shown in Fig.15. When $\xi_r = 0$ the current density becomes zero for the negative bias voltage since there is no electron to flow. As ξ_r increase, the IV curves become more symmetric. However, it can be observed that the shape of the IV curves does not change anymore when ξ_r is bigger than 3 eV because the added electrons have too low energy to move to the other side. Meanwhile, the other conditions are set to be the same for each calculation ($T = 300\ K$, $\xi_l = 2\ eV$, $a = 1\ nm$, $U_0 = 2\ eV$).

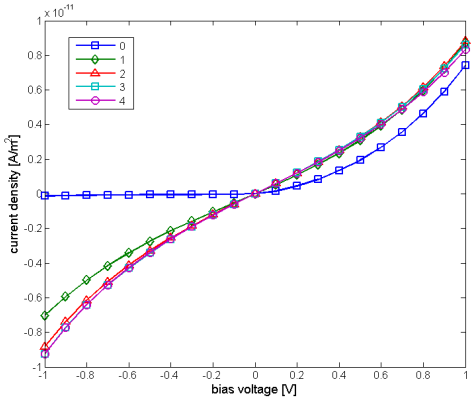

FIG. 15. IV curves for different ξ_r values(0-4 eV). When $\xi_r = 0$ the current density becomes zero for the negative bias voltage since there is no electron to flow, and as ξ_r increase IV curves become more symmetric.

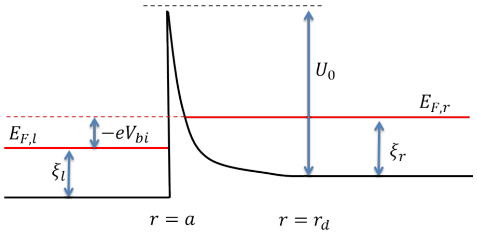

FIG. 16. Definition of parameters for the calculation of the Schottky barrier

B. Spherical Schottky Barrier

The parameters for the calculations are defined as below (See Fig.16) :

Barrier Height	U_0
Barrier Width	a
Fermi Energy on the Left/Right	$E_{F,l}/E_{F,r}$
Conduction Band Bottom on the Left/Right	$E_{C,l}/E_{C,r}$
$E_F - E_C$	ξ_l/ξ_r
Bias Voltage	V_{bi}

The first thing to note is that the dependence of the diode size, a (Should not be confused with the barrier thickness a in the previous section. In spherical Schottky barrier, the thickness of barrier is $r_d - a$.). In Fig.17, the IV curves were calculated for the diode sizes 10^{-11} m, 10^{-10} m, 10^{-9} m, and 10^{-8} m. The other conditions were set to be the same ($U_0 = 6$ eV, $\xi_l = \xi_r = 2$ eV, $T = 300$ K). It can be seen that as the diode size becomes smaller it comes to follow the Ohmic behavior while the curves have the bigger curvature when the barrier is thick. When the barrier is thick it is hard for electrons to penetrate by the tunneling, so electrons can tunnel through the barrier only when the high enough bias voltage is applied .

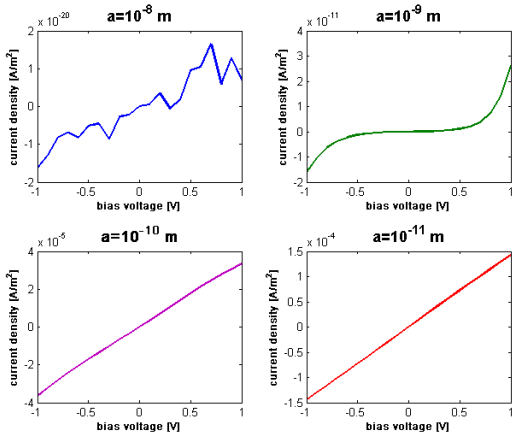

FIG. 17. IV curves for various values of barrier thickness. As the barrier thickness become smaller it becomes to follow Ohmic behavior while the curves have the more curvature when the barrier was thick.

The next thing to note is the temperature dependence of the IV curves (Fig.18). At low temperature regime the curvature of the curve is obvious while as the temperature becomes high it becomes linear. Here, the other conditions were set to be the same ($U_0 = 6$ eV, $\xi_l = \xi_r = 2$ eV, $a = 1$ nm). At low temperature, the electrons near the Fermi surface satisfy the interference condition, so the curvature in IV curves appears. On the other hand, when the temperature is high enough, most of the current comes from the thermionic emission. From this result, it can be induced that the tunneling contribution to the current is opposite to the usual diode behavior of Schottky barrier where only the thermionic emission is considered.

The interesting trend can be observed when we watch the barrier height dependence of the IV curves (Fig.19, 20). When the barrier height is low ($U_0 = 1$ eV) the IV curve is Ohmic, which is trivial because most of the current comes from the thermionic emission. As the barrier becomes higher up to 4 eV, the IV curves come to behave like a diode. A diode-like behavior of IV curve is easily explained as most semiconductor textbooks treat[4]. In Fig.4-(C) the electron has to overcome the barrier height $e\phi_{bn}$, while in Fig.4-(D) the electron only need to have a energy $e(\phi_{bi} - V)$, where only a thermionic contribution is considered. However, in the numerical calculation I included both of tunneling and thermionic emission. As the barrier height increases more, the reverse current starts to increase, and at $U_0 = 8$ eV the reverse current exceeds the forward current, thus reversing the rectifying behavior of the diode. In this regime, only the tunneling current is important and the thermionic contribution is exteremely small. Meanwhile, all the other conditions were set to be the same for each calculation ($T = 300$ K, $\xi_l = \xi_r = 2$ eV, $a = 1$ nm).

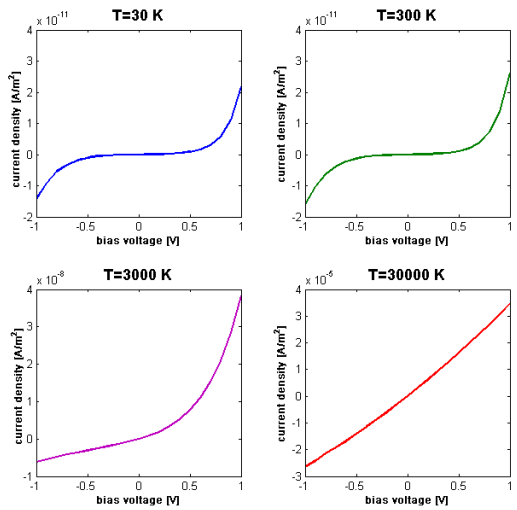

FIG. 18. The temperature dependence of the IV curves. At low temperature the tunneling current dominates the thermionic current, thereby the reverse current is observed. As the temperature becomes high the diode behavior starts to appear, and in extremely high temperature it eventually becomes Ohmic.

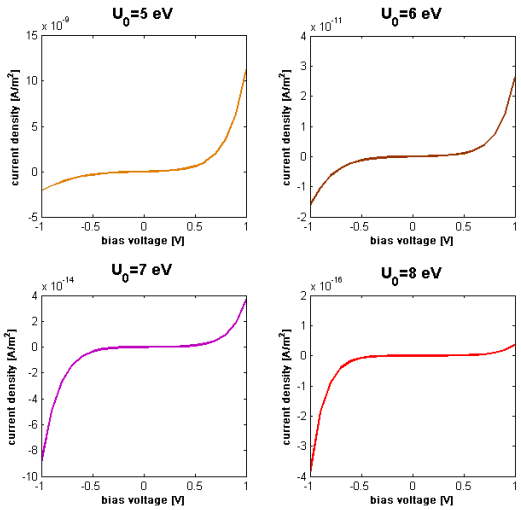

FIG. 20. The IV curves for the various barrie height values (large U_0 regime). As the barrier height becomes larger, the reverse current appears, thereby reversing the rectifying behavior of the Schottky diode.

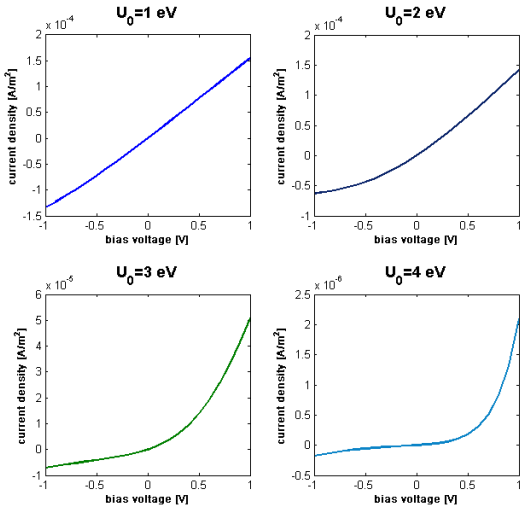

FIG. 19. IV curves for the various barrier height values (small U_0 regime). At $U_0 = 0$, it's Ohmic since almost all of the current comes from the thermionic emission. As the barrier height becomes larger, the diode-behavior is observed, which can be explained in the general terms like many other semiconductor textbooks.

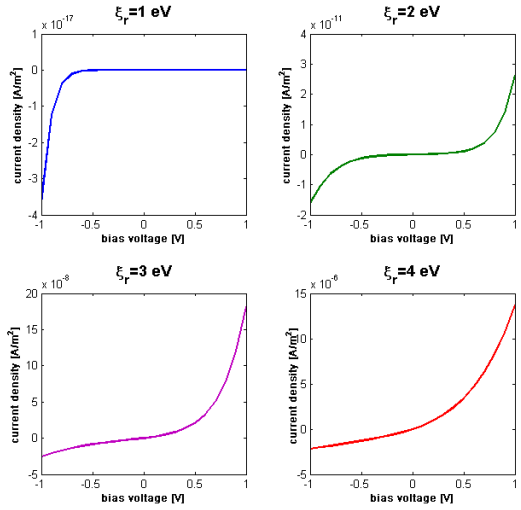

FIG. 21. IV curves for the various ξ_r values. At $\xi_r = 1\ eV$, IV curve is is opposite to the usual Schottky diode. In this regime the tunneling current dominates the thermionic current. As ξ_r increases, the thermionic emission current starts to contribute, thereby the diode-behavior starts to appear.

Finally, another interesting behavior is shown in IV curves for the different ξ_r values (Fig.21). The other conditions were set to be the same ($T = 300\ K$, $\xi_l = 2\ eV$, $a = 1\ nm$, $U_0 = 6\ eV$). At $\xi_r = 1\ eV$, rectifying behavior of the diode is reversed. The region is the same as the discussion before. When the tunneling contribution to the current dominates the thermionic contribution, the rectifying behavior is reversed. As the ξ_r value increases the thermionic current starts to contribute, thus the usual diode behavior of the Schottky barrier is observed.

CONCLUSION

In this paper, the contact between the metal tip and n-type semiconductor contact is modeled as a Schottky contact barrier. Using the depletion approximation, the Poisson equation was solved to get the shape of the potential barrier. Then, by plugging in the potential barrier calculated before, the Schrodinger equation was solved and the transmission coefficient was calculated. Finally, combined with the Fermi-Dirac function, the current density was calculated.

It was observed that when thermionic current dominates the tunneling current contribution (high T, large a, small U_0, large ξ) the IV curve just follows the usual diode behavior, which can be explained like many other semiconductor textbooks. However, when tunneling current dominates (low T, small a, large U_0, small ξ), the reverse current starts to appear and thereby reverse the rectifying behavior of the diode.

From the experimental result, it is suggested that the current at the tip is composed of both tunneling and thermionic current. Since the two contributions are mixed, it would show the half-like diode IV curve.

ACKNOWLEDGEMENT

I want to acknowledge my supervisor Univ.-Prof. Ph.D. Peter Hadley for supporting me for every aspects of this project, both theoretical and experimental. I also want to thank Stefan Kirnstötter for guiding me in the laboratory and supporting the experiments.

* godw2718@postech.ac.kr

[1] http://lamp.tu-graz.ac.at/~hadley/sem/index/index.php
[2] John G. Simmons, J. Appl. Phys. **34**, 1793 (1963)
[3] http://web.tiscali.it/decartes/phd_html/node3.html
[4] Juan Carlos Cuevas, Elke Scheer, *Molecular Electronics - an introducton to theory and experiment*, 2010
[4] Alexander Schnabel, Stephan Stoica, The report for the class *Electrical Measurement in a SEM*
[4] B. Ven Zeghbroeck, *Principles of Semiconductor Devices*, Online textbook, 2011
[5] G. D. Smit, S. Rogge, T. M. Klapwijk, Appl. Phys. Lett. **81**, 20 (2002)

APPENDIX

Here, the matlab source code for the numerical calculations is included.

A. Square Barrier

There are four function files named *schrodinger*, *tunneling*, *fermi*, and *current*. All these files should be in the same folder.

Function file for solving the Schrodinger equation

```
function dy=schrodinger(t,y)
dy=zeros(2,1);
global Ex a Vx V0 xsir

m=9.10938188*10^(-31);
hbar=(6.626068*10^(-34))/(2*pi);
e=1.60217646*10^(-19);

dy(1)=y(2);
dy(2)=y(1)*2*m
*((e*V0+xsir) - e*Vx*(1-t/a) - Ex)/(hbar^2);
```

Fermi function file

```
function [ f ] = fermi(E)
global Temp kB
f=1/(  exp(E/(kB*Temp)) + 1);
end
```

Function file that gives the current density for the energy level E - E+dE

```
function [dJ]=tunneling(V)
global e hbar E kB Temp Ex Vx V0 Vx a xsil xsir

e=1.60217646*10^(-19);
m=9.10938188*10^(-31);
h=6.626068*10^(-34);
hbar=(6.626068*10^(-34))/(2*pi);
kB=1.3806503*10^(-23);


a=1*10^(-11); %barrier depth
V0=3;% barrier hight

xsil=2*e; % filled electron in LHS
xsir=2*e; % filled electron in RHS

mul=xsir-e*V;
mur=xsir;
```

```
Temp=300; %device temperature


Vx=V;
VR=V;
N=100; %energy step

%ground energy
ger=0;
gel=-(xsil-xsir)-e*Vx;

if (gel<0)
    E=linspace(ger,max(mul,mur)+10*kB*Temp,N);
    dE=E(2)-E(1);
else
    E=linspace(gel,max(mul,mur)+10*kB*Temp,N);
    dE=E(2)-E(1);
end

kr=sqrt(2*m*E/(hbar)^2);
kl=sqrt(2*m*(E+xsil-xsir+e*Vx)/(hbar)^2);

Ai=zeros(N,1);
Ar=zeros(N,1);
T=zeros(N,1);
dJ=zeros(N,1);

for j=1:N
Ex=E(j);


[x psi]=ode45('schrodinger', [a 0]
,[exp(1i*kr(j)*a) 1i*kr(j)*exp(1i*kr(j)*a)]);
nn=size(x);
n=nn(1,1);

Ai(j)=(psi(n,1)+psi(n,2)/(1i*kl(j)))/2;
Ar(j)=(psi(n,1)-psi(n,2)/(1i*kl(j)))/2;

T(j)=1-(abs(Ar(j)/Ai(j)))^2;
T1=T(j);
dJ(j)=-(4*e/h)*T1*(fermi(Ex-mul)-fermi(Ex-mur))*dE;
end
end
```

Function File that gives the IV curve

```
function [V J]=current(Vspan,Vstep)
V=transpose(linspace(Vspan(1),Vspan(2), Vstep));
J=zeros(Vstep,1);
for j=1:1:Vstep
    J(j)=nansum(tunneling(V(j)));
end
figure
plot(V,J,'-o');
```

Schottky Barrier

There are four function files named *schrodinger1*, *tunneling1*, *fermi1*, and *current1*. All these files should be in the same folder.

Function file for solving the Schrodinger equation

```
function dy=schrodinger1(t,y)
dy=zeros(2,1);

global Ex rd

m=9.10938188*10^(-31);
hbar=(6.626068*10^(-34))/(2*pi);
e=1.60217646*10^(-19);
Nd=10^(21);
ep0=8.85418782*10^(-12);
epr=1;
ep=ep0*epr;
k=(e*Nd)/(6*ep);


dy(1)=y(2);
dy(2)=y(1)*2*m
*(-e*k*(3*(rd^2)-(t^2)-2*(rd^3)/t)-Ex)/(hbar^2);
```

Fermi function file

```
function [ f ] = fermi1(E)
global Temp kB
f=1/(  exp(E/(kB*Temp)) + 1);
end
```

Function file that gives the current density for the energy level E - E+dE

```
function [dJ]=tunneling1(V)
global kB Temp Ex Vx a rd

% fixed constants
e=1.60217646*10^(-19);
m=9.10938188*10^(-31);
hbar=(6.626068*10^(-34))/(2*pi);
h=6.626068*10^(-34);
kB=1.3806503*10^(-23);
ep0=8.85418782*10^(-12);
epr=1;
ep=ep0*epr;
Nd=10^(21);
```

```
k=(e*Nd)/(6*ep);


xsil=2*e; % chemical potential at LHS
xsir=2*e; % chemical potential at RHS

mul=xsir-e*V;
mur=xsir;

Temp=300; %device temperature
a=1*10^(-8);
Vs=-6;


Vx=V;
VR=V;

N=100; %energy step

rds=roots([2,-3*a,0,(a^3)+((Vs+Vx)*a/k)]);
rd=rds(1);

%ground energy
ger=0;
gel=-(xsil-xsir)-e*Vx;

if (gel<0)
    E=linspace(ger,max(mul,mur)+10*kB*Temp,N);
    dE=E(2)-E(1);
else
    E=linspace(gel,max(mul,mur)+10*kB*Temp,N);
    dE=E(2)-E(1);
end

kr=sqrt(2*m*E/(hbar)^2);
kl=sqrt(2*m*(E+xsil-xsir+e*Vx)/(hbar)^2);

Ai=zeros(N,1);
Ar=zeros(N,1);
T=zeros(N,1);
dJ=zeros(N,1);

for j=1:N
Ex=E(j);


[x psi]=ode15s('schrodinger1', [10*a a]
,[exp(1i*kr(j)*10*a) 1i*kr(j)*exp(1i*kr(j)*10*a)]);
nn=size(x);
n=nn(1,1);

Ai(j)=(psi(n,1)+psi(n,2)/(1i*kl(j)))/2;
Ar(j)=(psi(n,1)-psi(n,2)/(1i*kl(j)))/2;

T(j)=1-(abs(Ar(j)/Ai(j)))^2;
T1=T(j);
dJ(j)=-(4*e/h)*T1*(fermi1(Ex-mul)-fermi1(Ex-mur))*dE;
end
end
```

Function File that gives the IV curve

```
function [V J]=current1(Vspan,Vstep)
V=transpose(linspace(Vspan(1),Vspan(2), Vstep));
J=zeros(Vstep,1);

for j=1:1:Vstep
    J(j)=nansum(tunneling1(V(j)));
end
end
```